Nanoscale

Accepted Manuscript

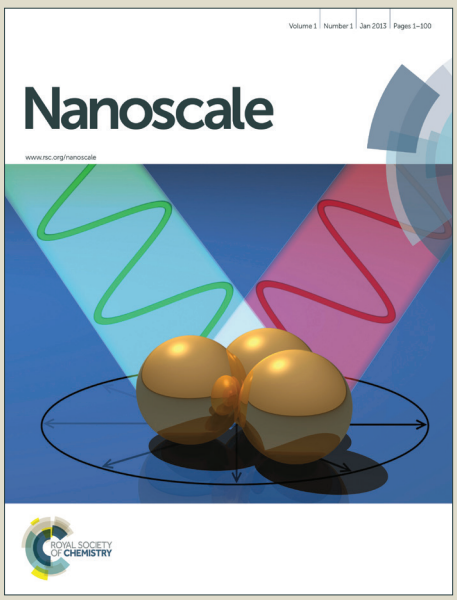

ROYAL SOCIETY OF CHEMISTRY

www.rsc.org/nanoscale

Cite this: DOI: 10.1039/c0xx00000x

www.rsc.org/xxxxxx

ARTICLE TYPE

Semipermeable Enzymatic Nanoreactor as an Efficient Modulator for Reversible pH Regulation

Yanyan Huang,[a,b] Youhui Lin,[a,b] Xiang Ran,[a,b] Jinsong Ren*[a] and Xiaogang Qu*[a]

Received (in XXX, XXX) Xth XXXXXXXXX 20XX, Accepted Xth XXXXXXXXX 20XX

DOI: 10.1039/b000000x

Here we proposed a new concept for the fabrication of a semipermeable enzymatic nanoreactor as an efficient modulator to reversibly switch the pH of the aqueous environment. We used amino functionalized expanded mesoporous silica nanoparticles (EMSN) as model nanocarrier to load enzymes. In order to protect enzymes from the interference of complicated environment, the polyelectrolyte multilayers (PEMs) were coated on the surface of EMSN through layer by layer (LbL) assembly. These PEMs could be served as semipermeable membrane, allowing small molecules diffusing in and out freely while trapping the enzymes in the nanoreactors. Compared with traditional electrochemical stimulation or optical control methods, our enzymatic regulation platform was easy to operate without complicated instruments. In addition, this system could cover a wide range of pH values and was convenient to regulate the pH values by simply controlling the concentrations of catalysts or reactants. Meanwhile, this strategy was general for other enzymes or other nanocarriers to achieve the reversible pH regulation for different purpose. The switched pH values could be implemented for the modulation of the conformational changes of nucleic acid and activation of the charge conversion in the drug delivery application.

1. Introduction

pH values play an important role in physical activities of organisms or microorganisms.[1,2] A variety of chemical and biological transformations are modulated by the pH of aqueous environment.[3,4] For example, numerous bio-transformations, such as biocatalyzed transformations, the denaturation of proteins, or the conformational switches of DNA, are controlled by the surrounding pH.[5-7] In addition to those transformations, some life activities must be implemented in a particular physiological pH environment.[1] Once the surrounding pH is not competent, those life activities can not be carried out successfully. Due to the crucial influence in the life system, a great deal of interests has been focused on the functions of pH in the biological external environment. For instance, pH changes were used to control the conformational transformations of some molecules in the application of controlled drug release systems.[8-11] Also, the pH-responsive feature of fluorescent chromophores was applied to develop logic systems.[12] To this end, efforts to control the pH changes of aqueous environment have been suggested.[7,13-17] For example, by using a bis-aniline-cross-linked AuNP composite, Willner et al demonstrated an electrochemically stimulated pH switch in aqueous media.[13] In addition, Liu's group applied a light-induced hydroxide ion emitter to reversibly control the pH changes.[17] Although promising, these approaches often suffered from some shortcomings, such as the requirement for precision instruments, relatively harsh reaction conditions and the small changes in pH values.[14-16] Therefore, there is an urgent need to develop novel, smart and effective approaches to achieve pH regulation.

Recently, owing to the advantages of convenient operation, short reaction period and tunability in catalytic activities, enzymes have attracted an explosion of interests.[18-21] The diverse and numerous biocatalytic reactions can generate acids or alkalis, leading to the pH changes of the surroundings.[22,23] For example, a biofuel cell was constructed recently by integrating enzymatic systems with pH-switchable oxygen electrode.[24] However, those enzymatic reactions were always in unconfined environment and the enzymes often suffered the difficulties in recovering and recycling.[18-24] A solution to this problem may be offered by the rapid development of nanoreactors. Nanoreactors, which miniaturize reaction containers to mimic natural reaction environment, hold great promise for improved chemical transformations by protecting catalysts against the interferences from external environment.[25-27] Within the confined space provided by the container, reactions could implement with higher selectivity or less side reactions.[27] Furthermore, with the assistance of nanoreactor, the encapsulated catalysts could achieve the recycling of enzymes without losing their activity. In the past decades, different approaches have been utilized to construct nanoreactors.[28-33] For instance, Hest and coworkers made use of block-copolymer amphiphiles to construct the polymersome-based nanoreactors. By using this system, they demonstrated the positional assembly of enzymes and a three-step cascade reaction was successfully implemented.[28] Inspired by these unique features, herein, we proposed a new concept for the fabrication of a semipermeable enzymatic nanoreactor as an

efficient modulator to reversibly switch the pH values of the aqueous environment. Compared with electrochemical or photochemical methods to control the pH, we showed that the pH can be altered over three units through enzymatic reactions. The switched pH values were implemented for the modulation of the conformational changes of nucleic acid and activation of the charge conversion in the drug delivery application.

2. Experimental section

2.1. Reagents and materials

Tetraethylorthosilicate (TEOS), sodium hydroxide, 2,2-azinobis (3-ethylbenzothiozoline)-6-sulfonic acid (ABTS), 1,3,5-trimethylbenzene and citraconic anhydride were purchased from Sigma-Aldrich. Glucose was obtained from Sinopharm Chemical Reagent Co. (Shanghai, China). Hydroxylamine, 3-aminopropyltriethoxysilane (APTES), N-cetyltrimethylammonium bromide (CTAB) and urea were obtained from Alfa Aesar. Glucose oxidase, horseradish peroxidase, and urease were purchased from Sangon Biotechnology Inc. (Shanghai, China). Chitosan (molecular weight = 5495.1, number-average molecular weight and Mw/Mn = 2.299) was obtained from Golden-shell Biochemical Co., LTD. The oligonucleotides used in this paper were synthesized by Sangon Biotechnology Inc. (Shanghai, China). All other reagents were of analytical reagent grade and used as received. Ultrapure water (18.2 MΩ; Millpore Co., USA) was used throughout the experiment.

2.2. Synthesis of expanded mesoporous silica nanoparticles (EMSN)

The MSN was first synthesized according to the literature with little modification. After that, added N-cetyltrimethylammonium bromide (CTAB, 0.50 g) to 240 mL of pure water. Sodium hydroxide (1.75 mL, 2 M) was dissolved in CTAB solution, followed by adjusting the solution temperature to 80 °C. TEOS (2.5 mL) was added by dropwise while continuously stirring. The mixture was allowed to stir for 3 h and white precipitates were obtained. The solid product was filtered, washed with deionized water and ethanol, and dried in air. EMSN was prepared according to a swelling agent incorporation method with a slight modification. Briefly, the as-synthesized MSN (0.50 g) were dispersed in ethanol (15 mL) and then sonicated for 30 min. After that, adding 30 mL of 1:1 mixture (v/v) of deionized water and 1, 3, 5- trimethylbenzene to the above solution. The mixture was placed in the autoclave, and kept at 140 °C for 24 h. The white powder was washed with ethanol and deionized water, respectively. To remove the surfactant template (CTAB), the white product was refluxed for 16 h in a solution of 1.00 mL of HCl (37%) and 50 mL of ethanol. Then, the product was washed with deionized water and methanol, and dried under vacuum. Next, amine modification of the silica surface was performed by suspending EMSN (200 mg) in a solution of APTES (1 mmol) in dry toluene (20 mL) and heating them under reflux for 24 h. The obtained products were then collected by vacuum filtration, washed thoroughly with toluene, and dried under vacuum.

2.3. Preparation of mesoporous silica-encapsulated enzymes

EMSN-GOx: EMSN (8 mg) were dispersed in 4 mL 10 mM phosphate buffer by sonication for 5 min, followed by the addition of GOx (4 mg). The mixed solution was stirred at 4 °C for 24 h. After that, the solution was centrifuged at 4,368×*g* for 8 minutes. The supernatant was used to determinate the loading efficiency of GOx while the solid in the bottom of the tube was washed twice with water.

EMSN-Ur: The preparation of EMSN-Ur was similar to EMSN-GOx. EMSN (8 mg) were dispersed in 4 mL 10 mM phosphate buffer by sonication for 5 min, followed by the addition of Ur (4 mg). The mixed solution was stirred at 4 °C for 24 h. After that, the solution was centrifuged at 4,368×*g* for 8 minutes. The supernatant was used to determinate of the concentration of Ur loaded in EMSN while the solid in the bottom of the tube was washed twice with water.

EMSN-GOx/Ur: EMSN (16 mg) were dispersed in 4 mL 10 mM phosphate buffer by sonication for 5 min, followed by the addition of Ur (4 mg) and GOx (4 mg). The mixed solution was stirred at 4 °C for 24 h. After that, the solution was centrifuged at 4,368×*g* for 8 minutes. The solid in the bottom of the tube was washed twice with water.

2.4. Preparation of PEM-EMSN-enzyme

A $(PDDA/PSS)_3$ film (six layers) was assembled by sequential dipping of the substrate into PDDA (1 mg/mL) and PSS (1 mg/mL) aqueous solutions for 30 min each until the desired number of bilayers was obtained. Every dipping was followed by sufficient buffer rinsing.

2.5. Glucose oxidation reaction and ABTS oxidation reaction

The reaction product, gluconic acid, was assayed by reaction with hydroxylamine and subsequent complex with Fe^{3+}, which led to a red complex with a major absorbance at 505 nm. In brief, 250 mL of solution 1 (5 mM EDTA and 0.15 mM triethylamine in water) and 25 mL of solution 2 (3 M NH_2OH in water) were added to the catalytic reaction solution. After 25 min of incubation, 125 mL of solution 3 (1 M HCl, 0.1 M $FeCl_3$, and 0.25 M CCl_3COOH in water) was added to the above aqueous solution, and the reaction was allowed to proceed for 5 min before spectral measurements. In experiments, the nanoparticles were centrifuged to prevent the influence of the absorbance of the nanoparticles to the colorimetric reaction. The other product, H_2O_2 was tested interrogated through the oxidation of ABTS in the presence of HRP. The oxidation product in 10 mM phosphate buffer (pH 7.4) produced a green color with major absorbance peaks at 417 nm.

2.6. Urea hydrolyzation detection

Ammonia, The product of urea hydrolysis, was detected by acid-base indicators (methyl red and phenolphthalein). We also used acid-base titration to determinate of the concentration of ammonia.

2.7. Preparation of citraconic anhydride conjugated chitosan (CS-Cit)

Chitosan (CS, 0.4 mg) was dissolved in 0.5 M $NaHCO_3$ buffer (pH 9.0, 25 mL). After that, the mixture was stirred at 4 °C for 30 min, and then added with citraconic anhydride (Cit, 1.39 g) slowly. The pH of the above solution was kept at 9.0 by adding with NaOH (0.1 M). After stirring for 24 h, the above solution

was purified dialysis (MWCO 3500) (×3 with distilled water). The final product (CS-Cit) was achieved by lyophilization.

2.8. Measurements and characterizations

TEM images and high-angle annular dark-field scanning TEM (HAADF-STEM) were recorded using a FEI TECNAI G2 20 high resolution transmission electron microscope operating at 200 kV. The hydrodynamic diameters and ζ-potentials of all examples were measured in a zeta sizer 3000HS analyzer. N_2 adsorption-desorption isotherms were recorded on a Micromeritics ASAP 2020M automated sorption analyzer. FTIR analysis was carried out on a Bruker Vertex 70 FT-IR Spectrometer. The pore size was determined following the BJH method. TGA was recorded with a RIGAKU Standard type with a heating rate of 10 °C min^{-1} from room temperature to 800 °C. The UV-Vis absorption spectra were recorded using a JASCO V550 UV/Visible spectrophotometer (JASCO International Co., LTD., Tokyo, Japan). The pH measurements were performed with a PHS-3C portable pH meter (Shanghai Precision & Scientific Instrument Co., China). CD spectra were measured on a JASCO J-810 spectropolarimeter. The optical chamber of CD spectrometer was deoxygenated with dry purified nitrogen (99.99%) for 45 min before use and kept the nitrogen atmosphere during experiments. Three scans were accumulated and automatically averaged.

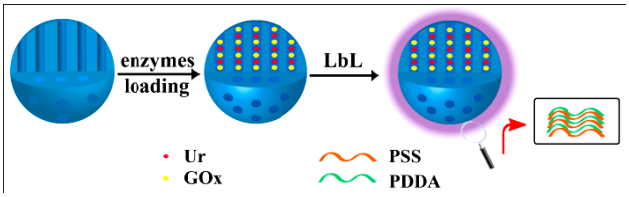

Scheme 1. Preparation processes of enzyme-based nanoreactors (PEM-EMSN-GOx/Ur).

3. Results and discussion

Due to the large surface area, high loading capabilities, tunable pore sizes and facile surface functionalization, mesoporous silica nanoparticles (MSN), as an ideal mesoporous material, has drawn widespread concern on the applications in medical and biological fields.[34-36] By taking advantage of these unique features, we used the amino functionalized expanded mesoporous silica nanoparticles (EMSN-NH_2) as a model container to load natural enzymes efficiently. The working principle was schematically represented in Scheme 1. In our system, glucose oxidase (GOx) and urease (Ur) were utilized as model enzymes to modulate the pH of aqueous solutions by catalyzing biological reactions. We loaded enzymes at 4 °C for 24 h. The mixture was then centrifuged and washed to remove the free enzyme. After that, polyelectrolyte multilayers (PEMs) were coated on the surface of EMSN through electrostatic adsorption. In our work, two typical polyelectrolytes, poly (styrene sulfonate) (PSS) and poly (diallyldimethylammonium chloride) (PDDA), were chosen for PEM construction.[37] The composites were noted as PEM-EMSN-enzyme. Importantly, the layer by layer assembly of PEMs could serve as a semipermeable membrane, enabling small molecules diffusing in and out freely while trapping the enzymes in the nanoreactors.[28,38] Compared with free enzymes, encapsulating enzymes in nanoreactors allowed the enzymes to be easily recovered from the reaction mixture. It was worth noting that, without significant compromise of enzyme activity, our system showed the advantages of effectively stabilizing enzymes in the complicated environment as well as protecting them against protease attack.

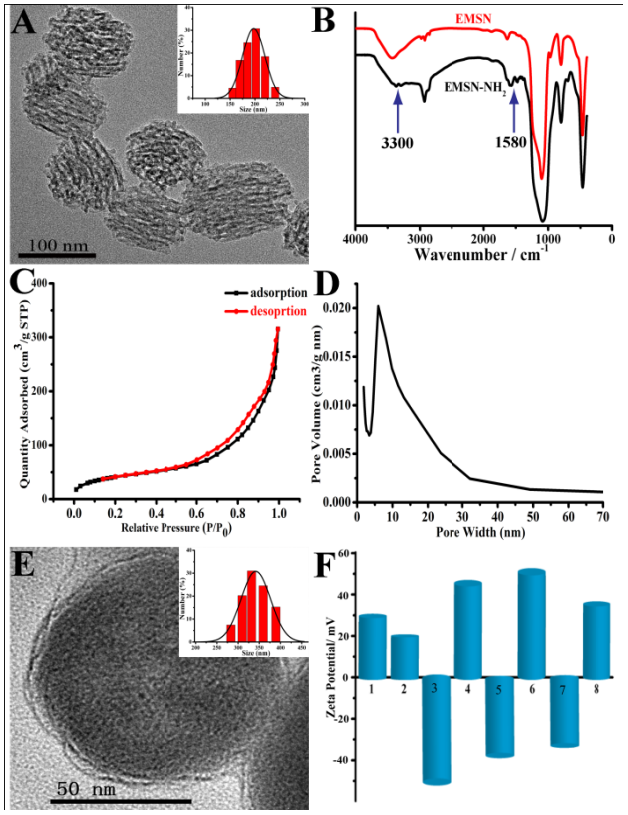

Fig. 1 A) TEM image of the expanded mesoporous silica nanoparticles, inset was the diameter distribution by DLS test; B) FT-IR spectra of EMSN and the amino functionalized EMSN nanoparticles; C) N_2 adsorption-desorption isotherms of EMSN; D) pore-size distribution curve of EMSN; E) TEM images of PEM-EMSN-Ur/GOx, inset was the diameter distribution by DLS test; F) ζ potentials of the nanoreactors at different processes: 1) EMSN; 2) EMSN and enzymes incubated for 24 h in 4 °C; 3-8) Different periods (one layer, two layers, three layers, four layers, five layers and six layers respectively) of polymers coated around EMSN.

To demonstrate the feasibility of our protocol, EMSN was first synthesized according to the previously reported progress.[39-41] The formation of large-pore nanoparticle was verified with transmission electron microscopy (TEM) measurements shown in Fig. 1A. The resultant EMSN could be well dispersed in the aqueous solution and the hydrodynamic diameters of the EMSN was measured using dynamic light scattering (DLS). The nanoparticle had a uniform diameter of 200 nm with a narrow particle size distribution (Fig. 1A, inset). N_2 adsorption-desorption isotherms of EMSN showed a typical Type IV curve with a specific surface area of 148.1 m^2/g, average porous diameter of 9.5 nm and a narrow pore distribution (Fig. 1C and 1D). Therefore, the expanded mesoporous silica nanoparticles could be used to encapsulate enzymes effectively. Before assembling with PEMs, the amino group was first modified on

the surface of EMSN. Fig. 1B was the FT-IR spectra of the amino functionalized expanded mesoporous silica nanoparticles. The successful grafting of amino group onto the mesoporous silica was validated by the appearance of absorption band around 3300 cm^{-1} and 1580 cm^{-1}, which are assigned to the N-H stretching vibration and bending vibration, respectively. After assembling with six polymers layers, the PEM-EMSN-GOx/Ur nanoreactor had a hydrodynamic size of about 340 nm and the size distribution became broadened (Fig. 1E, inset). As displayed in the corresponding TEM image, there was a uniform thin layer absorbed around the surface of the EMSN (Fig. 1E). In comparison with the size observed from TEM images, after modified with these hydrated groups and layers, the diameters of mesoporous silica nanoparticles based on DLS became much larger due to the swell in aqueous solution (Figure 1A and 1E).[42-44] To further confirm the successful assembling of polymer layers, the surface charges of the nanoreactors were determined by measuring their ζ potentials. As displayed in Fig. 1F, after assembling, the final ζ potential of the complex was around 35 mV which was consistent with our hypothesis. In order to more quantitatively evaluate the amount of PEMs attached, the complex was subjected to thermogravimetric analysis (TGA) in air at a heating rate of 10 °C/min. As demonstrated in Fig. S1, there was 17.32% weight loss up till 800 °C corresponds to the desorption and decomposition of the PEMs. As a semipermeable system, this nanoreactor could efficiently protect the inner enzymes from the attacking of protease. To verify our hypothesis, enzyme hydrolysis experiment was carried out. Protease K and GOx were chosen as the model protease and enzyme, respectively. As shown in Fig. S2, the PEM-EMSN-GOx nanoreactor remained almost 95% activity after incubated with protease for 24 h while free GOx lost more than 60% activity. This result demonstrated that our system can indeed protect the inner enzymes against the interference of external environment. Taking together, all these findings fully illustrated our approach was able to construct the enzyme-based nanoreactors.

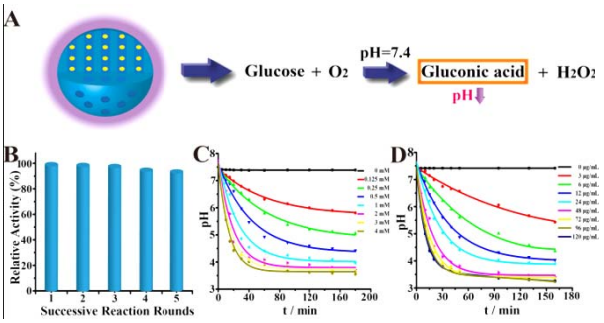

Fig. 2 A) Schematic illustration for the catalytic activity of PEM-EMSN-GOx; B) The circulation utilization rate of the nanoreactors, each circle was incubated for 20 min in 37 °C and then added 1 mM ABTS and 0.05 μg/mL HRP to the mixed solution; C) Time-dependent pH changes in the presence of different concentrations of substrate glucose from 0 to 4 mM; D) Time-dependent pH changes in the presence of different concentrations of catalyst from 0 to 120 μg/mL. All the reactions are carried out in 0.5 mM pH 7.4 phosphate buffer.

In order to investigate the proof of principle of the composite components, we first loaded GOx in EMSN. The loading efficiency was measured by determining the UV absorption at 280 nm and it reached around 80% (Fig. S3). After that, we evaluated the activities of nanoparticles individually. It's well known that GOx can catalyze the oxidation of glucose to generate gluconic acid with the decreasing of pH values of the environment (Fig. 2A).[22] Therefore, we validated the reaction products and the resulting solution was interrogated with a gluconic acid specific colorimetric assay in the presence of Fe^{3+} and hydroxylamine.[45] As shown in Fig. S4, in the presence of all reaction components, the color of the solution turned red immediately. Control experiments indicated that neither glucose nor the catalyst alone could induce any visual changes. Furthermore, the production of gluconic acid in the system might decrease the surrounding pH, which would play an essential role in our system. In order to monitor the pH changes of the mixed solution, we used methyl red as a pH indicator. Before testing, it was necessary to demonstrate the influence of buffer concentrations on enzymatic reactions (Fig. S5). In high concentration, the pH value of environment was almost invariable while in low concentration there was a dramatic decrease of pH value. This phenomenon was consistent with the buffer capacity. Therefore, we chose 0.5 mM phosphate buffer as the reaction environment. Fig. S6 was the control experiment of acid generation. As the figure displayed, neither the reactant nor the catalyst alone could introduce any color change. In contrast, an obvious yellow to red color change was observed after incubating glucose with the catalyst, demonstrating the pH value of the system was changed from 7.4 down to around 4. Experimental results confirmed that gluconic acid was indeed produced in this enzyme catalyzed reaction. The other product, H_2O_2, was interrogated through chromogenic reaction with the addition of 2,2-azinobis (3-ethylbenzothiozoline)-6-sulfonic acid (ABTS) and horseradish peroxidase (HRP). In the presence of HRP, as expected, H_2O_2 could oxidase ABTS to produce a colored product $ABTS^{\cdot+}$ while no obvious color changes were obtained in other conditions (Fig. S7).[46] Further studies demonstrated that our nanoreactors had distinctive advantages to control the pH changes by regulating the concentration of the reaction substrate (Fig. 2C) or the catalyst (Fig. 2D). The regulation of pH change could also be obtained through controlling reaction times. As displayed in Fig. 2C and 2D, the pH of all solutions decreased as the time going. When increasing the concentrations of catalyst or reactant, differences of the above solutions in pH changes were more apparent. Taken together, these results conformed that our enzyme-based nanoreactors could modulate the pH changes of aqueous solution flexibly. It was noteworthy that, our catalyst still maintained about 95% activities over the course of five rounds of reaction, demonstrating a high durability (Fig. 2B). Therefore, the excellent durability endowed our nanoreactor for long-term operating.

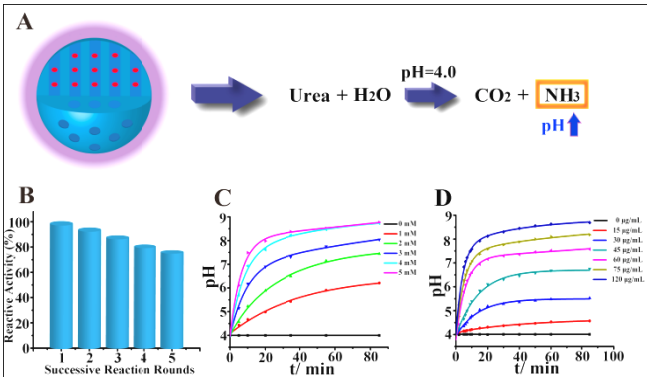

Fig. 3 A) Schematic illustration for the catalytic activity of PEM-EMSN-Ur; B) The circulation utilization rate of the nanoreactor, each circle was incubated for 20 min in 37 °C and then titrated with 25 mM HCl. Methyl red was used as the acid-base indicator; C) Time-dependent pH changes in the presence of different concentrations of substrate urea from 0 to 5 mM; D) Time-dependent pH changes in the presence of different concentrations of catalyst from 0 to 120 μg/mL. All the reactions are carried out in 0.5 mM pH 4.0 phosphate buffer.

Ur is a natural enzyme widely distributed in the plant seed, some also present in animal blood and urine. It is capable of catalyzing the hydrolysis of urea to produce alkaline substance, ammonia and gradually tunes the local pH (Fig. 3A).[23] We first prepared the PEM-EMSN-Ur complex and then investigated the activities. The loading efficiency of Ur was calculated by UV absorption spectrum analysis method and it was around 50% (Fig. S8). Fig. S9 displayed the pH changes of different combinations. When PEM-EMSN-Ur was incubated with urea in pH 4.0 phosphate buffer, the pH of solution soon increased as ammonia was generating gradually. The solution could tune a color change of phenolphthalein from colorless to red (Fig. S10), while no obvious color change could be seen by other combinations. We also used methyl red to detect pH changes. When PEM-EMSN-Ur and urea were both present in solution, after incubating for about 1 h, an obvious red to yellow color switch was observed (Fig. S10). The above results proved our hypothesis that PEM-EMSN-Ur could catalyze the hydrolysis reaction and increase the pH values. The influences of catalyst or substrate concentrations were shown in Fig. 3C and 3D, respectively. The results clearly confirmed that the pH changes could also be modulated through controlling the concentrations of catalyst or reactant. The durability of urease-based nanoreactor was also studied and it still remained near 80% activity after five cycles (Fig. 3B), conforming that this nanoreactor could be used for a long time.

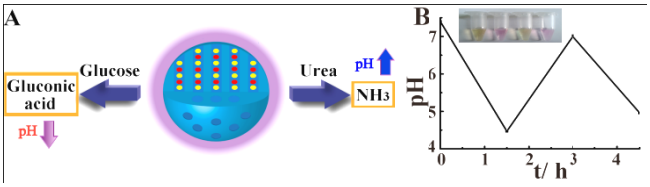

Fig. 4 A) The scheme of overall reaction; B) Reversible pH changes after adding glucose or urea in different periods. Inset was the photograph of different periods.

The flexible pH regulating capability of single-enzyme system prompted us to evaluate the feasibility of using two-enzyme system to regulate pH changes reversibly. The scheme of integrated reactions was depicted in Fig. 4A and the composite catalyst was incubated in phosphate buffer initially (pH=7.4). When 1 mM glucose was added to the solution, the surrounding pH would decrease to near 4.4. After that, 1.25 mM urea was added to the above solution. As a result, the pH value rose gradually and increased to above 7.0 (Fig. 4B). The results indicated that our nanoreactors could achieve reversible pH regulation. In addition, it was convenient for the system to modulate the pH by controlling the concentrations of catalysts and substrates or reaction times. Therefore, the reversible pH regulation and controllable pH changes meet the requirements for constructing smart pH regulating device.

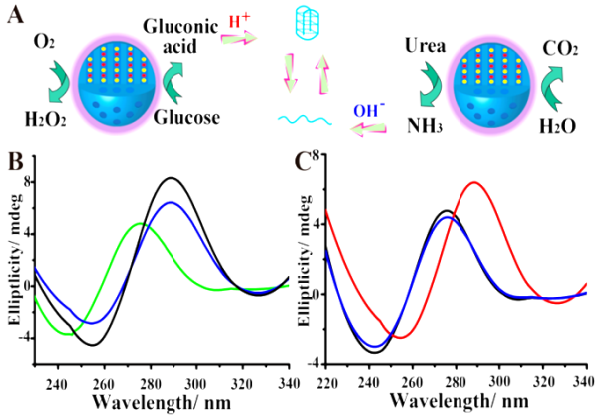

Fig. 5 A) The scheme of conformational changes of i-motif DNA; B,C) CD spectra of the i-motif DNA after addition of the reaction mixture; (B) CD spectra of the i-motif DNA after addition of the reaction mixture from acid environment to base surroundings and finally back to acid solution: pH 4.0 phosphate buffer (black line), then adding PEM-EMSN-GOx/Ur and urea for 2 h in 37 °C (green line), followed by adding PEM-EMSN-GOx/Ur and glucose for 2 h in 37 °C (blue line); (C) CD spectra of the i-motif DNA after addition of the reaction mixture from basic environment to acid surroundings and finally back to basic solution: pH 7.4 phosphate buffer (blue line), then adding PEM-EMSN-GOx/Ur and glucose or 2 h in 37 °C (red line), followed by adding PEM-EMSN-GOx/Ur and urea for 2 h in 37 °C (black line).

The successful cyclic pH changes induced by enzymatic reactions allow, in principle, controlling and switching of the reactivity of chemical or biological processes. To exemplify such processes, we selected i-motif DNA, as a model system. As one of the most studied DNA systems, i-motif DNA has now become a particularly promising candidate in nanostructure fabrication and nanodevice design.[6,47] Under slightly acidic condition, DNA strands with stretches of cytosine bases can form closely packed four-stranded structures called the "i-motif" through protonated cytosine–cytosine ($C:C^+$) base-pair formation.[48,49] Based on this phenomenon, a 22-mer C-rich DNA was used in our work (Fig. 5A). Fig. 5B and 5C were the circular dichroism (CD) spectroscopy of conformational switch of i-motif DNA in different conditions. As shown in Fig. 5C, in the initial neutral phosphate buffer environment (pH=7.4), C-rich DNA had a negative band centered at 250 nm and a major positive band at 273 nm, this revealed DNA was in an unstructured single strand structure. When this DNA was incubated in slightly acidic condition, a dramatic change was observed with a positive band near 287 nm and a negative band near 256 nm, which were characteristics of i-motif DNA. After the hydrolysis of urea, the pH of the solution increased to above 7.4 and this i-motif structure would deform into random coils with deprotonation of

the C:C$^+$ base pairs. We also evaluated the opposite experiment as was demonstrated in Fig. 5B. In order to eliminate the interference of nanoparticles, all solutions were centrifuged before CD measurements. The above results confirmed that our enzyme-based system could regulate the structural switch of i-motif DNA reversibly. As we have mentioned before, the conformational transformation of DNA has physiological significance and is widely applied in DNA-nanomachine design. Therefore, we hope our method will benefit the application of smart devices or materials, allowing the development of new strategies for constructing new types of responsive systems or biosensors in the future.

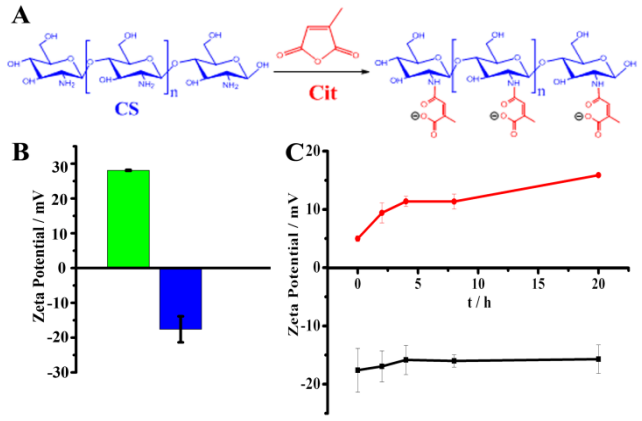

Fig. 6 A) The preparation process of CS-Cit; B) The ζ potential of the EMSN (green) and EMSN/CS-Cit (blue); C) The ζ potential of EMSN/CS-Cit at 25 °C as a function of time at different pH values: pH 4.5 (red) and pH 7.4 (black).

Furthermore, many other pH-dependent chemical transformations could be also activated by our enzyme-based nanoreactor. Recently, some polymer nanoparticles which have specific property of charge reversal in reaction to external pH stimuli have attracted an explosion of interests.[50,51] When the surrounding pH dropped from neutral to acid, their charge would have a negative-to-positive reversal. Taking advantage of this unique feature, this kind of charge-reversal nanoparticle holds great promise in drug delivery for cancer chemotherapy. As one of the charge reversal materials, citraconic anhydride (Cit) can easily react with chitosan (CS) to form amide (Fig. 6A).[52] The efficient pH regulation ability of our enzyme-based nanoreactor promotes us to explore its potential in controlling the charge conversion ability of these special polymers. In our experiment, we used CS-Cit modified EMSN-NH_2 as a model charge reversal nanoparticle to verify our hypothesis. CS-Cit was synthesized through our previous approach[52] and then adsorbed on the surface of EMSN through electrostatic interaction. Accordingly, the charge reversal behavior of this nanomaterial was evaluated by measuring their ζ potentials. As was shown in Fig. 6B, EMSN was positively charged under neutral conditions. After modified with negatively charged CS-Cit, the ζ potential turned to be negative. This result indicated the successful adsorption of CS-Cit on the surface of EMSN. We then monitored the time-dependence of the ζ potential of EMSN/CS-Cit at different pH values (neutral and acid). To produce an acidic solution, we incubated 120 μg/mL PEM-EMSN-GOx nanoreactor with 1 mM glucose for 1 h and the final pH value dropped to around 4.5. As shown in Fig. 6C, due to the presence of COOH group, the CS-Cit maintained a ζ potential of about -15 mV after incubation at pH 7.4 for 20 h. While at pH 4.5, they immediately became positively charged owing to the hydrolysis of Cit. After 20 h incubating, CS-Cit reached a ζ potential of about 16 mV. These findings demonstrated that the enzyme-based nanoreactor could successfully induce this polymer to convert their charge which may promote the development of nuclear drug delivery system.

4. Conclusions

In conclusion, our present work proposed a conceptually new approach of an efficient nanoreactor to achieve reversible pH regulation based on the enzymatic reactions. Compared with traditional methods, this nanoreactor had several outstanding advantages. First, the platform was simple to synthesize, easy to operate, and the enzyme-based nanoreactor could be used for long-term operating or repeated use. Second, our system could cover a wide range of pH values and control the pH changes more easily. Third, it was convenient to regulate the pH values by simply controlling the concentrations of catalysts or reactants. Meanwhile, this strategy was general for other enzymes or other nanocarriers to achieve the reversible pH regulation for different applications. More importantly, we have extended the use of our nanoreactor to reversibly modulate the conformational switches of i-motif DNA which may have potential applications in the construction of novel DNA nanodevices and biosensors. We also showed that our system could be utilized in activation of the charge conversion in the drug delivery application. We envision that our new findings may pave the way to construct novel nanoreactor with versatile functionalities, and will be highly beneficial for a wide range of applications including food technology, industrial production and environmental treatment.

Acknowledgements

Financial support was provided by the National Basic Research Program of China (Grant 2012CB720602, 2011CB936004) and the National Natural Science Foundation of China (Grants 91213302, 21210002).

Notes and references

[a] *Laboratory of Chemical Biology and State Key Laboratory of Rare Earth Resource Utilization, Changchun Institute of Applied Chemistry, Changchun, Jilin 130022 (China). E-mail: jren@ciac.ac.cn; xqu@ciac.ac.cn*
[b] *University of the Chinese Academy of Sciences, Beijing 100039 (China).*
† Electronic Supplementary Information (ESI) available: [Fig. S1-S10]. See DOI: 10.1039/b000000x/

1 M. A. Gock, A. D. Hocking, J. I. Pitt and P. G. Poulos, *Int. J. Food. Microbiol.*, 2003, **2481**, 11.
2 G. W. Nicol, S. Leininger, C. Schleper and J. I. Prosser, *Environ. Microbiol.*, 2008, **10**, 2966.
3 A. K. Dutta, S. Das, S. Samanta, P. K. Samanta, B. Adhikary and P. Biswas, *Talanta*, 2013, **107**, 361.
4 M. C. Williams, J. R. Wenner, I. Rouzina and V. A. Bloomfield, *Biophys. J.*, 2001, **80**, 874.
5 W. T. Jenkins and I. W. Sizer, *J. Biol. Chem.*, 1959, **234**, 1179.
6 D. Liu, E. Cheng and Z. Yang, *NPG. Asia. Mater.*, 2011, **3**, 109.
7 S. Kohse, A. Neubauer, A. Pazidis, S. Lochbrunner and U. Kragl, *J. Am. Chem. Soc.*, 2013, **135**, 9407.

8 X. Li, Q. He and J. Shi, *ACS Nano*, 2014, **8**, 1309.
9 K. Liang, J. J. Richardson, H. Ejima, G. K. Such, J. W. Cui and F. Caruso, *Adv. Mater.*, 2014, **26**, 2398.
10 X. Xue, Y. Zhao, L. Dai, X. Zhang, X. Hao, C. Zhang, S. Huo, J. Liu, C. Liu, A. Kumar, W. Chen, G. Zou and X. Liang, *Adv. Mater.*, 2014, **26**, 712.
11 P. Shi, K. Qu, J. Wang, M. Li, J. Ren and X. Qu, *Chem. Commun.*, 2012, **48**, 7640.
12 S. Silvi, E. C. Constable, C. E. Housecroft, J. E. Beves, E. L. Dunphy, M. Tomasulo, F. M. Raymo and A. Credi, *Chem.--Eur. J.*, 2009, **15**, 178.
13 M. Frasconi, R. T. Vered, J. Elbaz and I. Willner, *J. Am. Chem. Soc.*, 2010, **132**, 2029.
14 K. Morimoto, M. Toya, J. Fukuda and H. Suzuki, *Anal. Chem.*, 2008, **80**, 905.
15 L. T. H. Kao, H. Y. Hsu and M. Gratzl, *Anal. Chem.*, 2008, **80**, 4065.
16 S. Silvi, A. Arduini, A. Pochini, A. Secchi, M. Tomasulo, F. M. Raymo, M. Baroncini and A. Credi, *J. Am. Chem. Soc.*, 2007, **129**, 13378.
17 H. Liu, Y. Xu, F. Li, Y. Yang, W. Wang, Y. Song and D. Liu, *Angew. Chem. Int. Ed.*, 2007, **46**, 2515.
18 M. Liu, J. Fu, C. Hejesen, Y. Yang, N. W. Woodbury, K. Gothelf, Y. Liu and H. Yan, *Nat. Commun.*, 2013, DOI: 10.1038/ncomms3127.
19 M. De, S. S. Chou and V. P. Dravid, *J. Am. Chem. Soc.*, 2011, **133**, 17524.
20 Y. Weizmann, Z. Cheglakov and I. Willner, *J. Am. Chem. Soc.*, 2008, **130**, 17224.
21 R. Wolfenden and M. J. Snider, *Acc. Chem. Res.*, 2001, **34**, 938.
22 J. Fu, M. Liu, Y. Liu, N. W. Woodbury and H. Yan, *J. Am. Chem. Soc.*, 2012, **134**, 5516.
23 R. de. la. Rica and H. Matsui, *Angew. Chem. Int. Ed.*, 2008, **47**, 5415.
24 L. Amir, T. K. Tam, M. Pita, M. M. Meijler, L. Alfonta and E. Katz, *J. Am. Chem. Soc.*, 2009, **131**, 826.
25 D. M. Vriezema, M. C. Aragones, J. A. A. W. Elemans, J. J. L. M. Cornelissen, A. E. Rowan and R. J. M. Nolte, *Chem. Rev.*, 2005, **105**, 1445.
26 K. T. Kim, J. J. L. M. Cornelissen, R. J. M. Nolte and J. C. M. van. Hest, *Adv. Mater.*, 2009, **21**, 2787.
27 M. Spulber, A. Najer, K. Winkelbach, O. Glaied, M. Waser, U. Pieles, W. Meier and N. Bruns, *J. Am. Chem. Soc.*, 2013, **135**, 9204.
28 D. M. Vriezema, P. M. L. Garcia, N. S. Oltra, N. S. Hatzakis, S. M. Kuiper, R. J . M. Nolte, A. E. Rowan and J. C. M. van. Hest, *Angew. Chem. Int. Ed.*, 2007, **46**, 7378.
29 G. Delaittre, I. C. Reynhout, J. J. L. M. Cornelissen and R. J. M. Nolte, *Chem.--Eur. J.*, 2009, **15**, 12600.
30 C. V. Vazquez, B. Vaz, V. Giannini, M. P. Lorenzo, R. A. A. Puebla and M. A. C. Duarte, *J. Am. Chem. Soc.*, 2013, **135**, 13616.
31 H. A. Hoppe, F. Stadler, O. Oeckler and W. Schnick, *Angew. Chem. Int. Ed.*, 2004, **43**, 5540.
32 A. J. Zarur and J. Y. Ying, *Nature*, 2000, **403**, 65.
33 M. Xue and J. I. Zink, *J. Am. Chem. Soc.*, 2013, **135**, 17659.
34 Z. Li, Y. Tao, S. Huang, N. Gao, J. Ren and X. Qu, *Chem. Commun.*, 2013, **49**, 7129.
35 X. Yang , X. Liu , Z. Liu , F. Pu , J. Ren and X. Qu, *Adv. Mater.*, 2012**, 24**, 2890.
36 S. Angelos, Y. Yang, N. M. Khashab, J. F. Stoddart and J. I. Zink, *J. Am. Chem. Soc.*, 2009, **131**, 11344.
37 X. Zhang and Z. Su, *Adv. Mater.*, 2012, **24**, 4574.
38 Y. Lvov and F. Caruso, *Anal. Chem.*, 2001, **73**, 4212.
39 S. Huh, J. W. Wiench, J. C. Yoo, M. Pruski and V. S. Y. Lin, *Chem. Mater.*, 2003, **15**, 4247.
40 M. H. Kim, H. K. Na, Y. K. Kim, S. R. Ryoo, H. S Cho, K. E. Lee, H. Jeon, R. Ryoo and D. H. Min, *ACS Nano*, 2011, **5**, 3568.
41 S. Angelos, N. M. Khashab, Y. Yang, A. Trabolsi, H. A Khatib, J. F. Stoddart and J. I. Zink, *J. Am. Chem. Soc.*, 2009, **131**, 12912.
42 W. Huang, G. L. Davies and J. J. Davis, *Chem. Eur. J.*, 2013, **19**, 17891.
43 X. He, Y. Zhao, D. He, K. Wang, F. Xu and J. Tang, *Langmuir*, 2012, **28**, 12909.
44 F. Chen, H. Hong, Y. Zhang, H. F. Valdovinos, S. Shi, G. S. Kwon, C. P. Theuer, T. E. Barnhart and W. Cai, *ACS Nano*, 2013, **7**, 9027.
45 E. T. Rakitzis and P. Papandreou, *Chem.--Biol. Interact.*, 1998**, 113**, 205.
46 J. Li, S. Song, X. Liu, L. Wang, D. Pan, Q. Huang, Y. Zhao and C. Fan, *Adv. Mater.*, 2008, **20**, 497.
47 Y. Dong, Z. Yang and D. Liu, *Acc. Chem. Res.*, 2014, DOI:10.1021/ar500073a.
48 W. Li, L. Feng, J. Ren, L. Wu and X. Qu, *Chem--Eur. J.*, 2012**, 18**, 12637.
49 J. L. Leroy, M. Gueron, J. L. Mergny and C. Helene, *Nucleic Acids Res.*, 1994, **22**, 1600.
50 P. Xu, E. A. V. Kirk, Y. Zhan, W. J. Murdoch, M. Radosz and Y. Shen, *Angew. Chem. Int. Ed.*, 2007**, 46**, 4999.
51 Z. Zhou, Y. Shen, J. Tang, M. Fan, E. A. V. Kirk, W. J. Murdoch and M. Radosz, *Adv. Funct. Mater.*, 2009, **19**, 3580.
52 Z. Li, K. Dong, S. Huang, E. Ju, Z. Liu, M. Yin, J. Ren and X. Qu, *Adv. Funct. Mater.*, 2014, **24**, 3612.